

Casting technology for ODS steels - the internal oxidation approach

S Miran, P Franke, A Möslang, H J Seifert

Institute for Applied Materials - Applied Materials Physics, Karlsruhe Institute of Technology, 76344 Eggenstein-Leopoldshafen, Germany

Syedhossein.miran@kit.edu

Abstract. The formation of stainless ODS steel by internal oxidation of as-cast steel has been investigated. An alloy (Fe-16Cr-0.2Al-0.05Y, wt.%) was embedded in a (VO/V₂O₃) powder mixture serving as an oxygen activity buffer and heat treated at 1450 °C for 20 h. After this procedure no oxide scale was present on the surface of the sample but a zone of internal oxidation with a depth of about 2000 µm was formed in its interior. The precipitates within this zone consisted of two types of oxides. Discrete aluminium oxide particles with a size of a few micrometres were formed in outer regions of the specimen. Finer aluminium-yttrium oxides with a size of some hundred nanometres were mainly precipitated in inner regions of the sample. The results can be considered as a promising step towards an alternative production route for ODS steels.

1. Introduction

Reduced activation ferritic-martensitic (RAFM) steels are promising candidate materials for structural applications in fusion reactors. These steels have been developed based on massive industrial experiences of ferritic/martensitic steel [1]. RAFM steels have interesting properties such as low sensitivity to irradiation-induced swelling and helium embrittlement [2].

RAFM steels are very attractive structural materials but their high-temperature strength is limited and one of the effective approaches to solve this issue is oxide dispersion strengthening (ODS) method [3]. The nano-sized oxide particles with high number density can act as pinning points to dislocation movement [4]. Dispersed nano-sized oxides may provide a large number of trap sites for transmutant helium and radiation-induced defects [5]. The improved creep resistance and fatigue strength at high temperatures is another advantage of ODS steels [6].

The typical procedure for manufacturing ODS steels is the powder metallurgy route in which steel powders and Y₂O₃ powders are mechanically alloyed by high energy milling. The input oxides remain unmixed but they are dispersed throughout the microstructure of the alloy [7]. This technique was first developed by J. S. Benjamin and published in 1970 [8].

The next step in this route is hot isostatic pressing (HIP). In HIP process, the simultaneous application of a high pressure at elevated temperatures in a constructed vessel is planned for hot compaction of the powders. The pressure inside HIP chamber is generated usually by applying purified argon gas. In the later steps after HIP, the deformed powders are hot extruded or rolled for the desired shape.



Although this method for ODS steels is well documented, it is considered a complex and costly fabrication technique [9, 10]. In the present study an alternative process for the production of stainless ODS steels has been investigated. Firstly, homogeneous steel was prepared from the melt and in a subsequent step a dispersion of oxide particles was precipitated by internal oxidation in the solid state.

2. Background

Internal oxidation means the fabrication of oxides in the interior of an alloy, and more specific in the context of the present work, that the growth of an external oxide scale at the surface of the sample is avoided. A quantitative description of the internal oxidation has been given by Wagner [11], especially for the case of binary alloys where a less-noble metal (here Al) forms a dilute solution in the more noble matrix metal (here Fe). An English review of this theory has been given by Rapp [12].

For the occurrence of internal oxidation several requirements need to be fulfilled: the oxide of the less-noble element must have a strong negative Gibbs energy of formation, the diffusion of oxygen from the surface of the alloy into the interior must be faster than the diffusion of the less-noble metal into the opposite direction, and the concentration of oxygen in the alloy at its surface should be much smaller than the initial concentration of the less-noble metal [11]. Although the present investigation considers a four-component alloy, these criteria remain basically valid when Al and Y are considered as the less-noble components.

In the current work, the internal oxidation of a selected alloy of Fe-Cr-Al-Y has been investigated. The primary goal for this research is to provide a simple and fairly inexpensive method to disperse oxide particles on the matrix of steel.

The oxidation behavior of the main involved elements (Fe: main component, Cr: alloying element, Al and Y: oxide-forming elements) is a key concept for the successful internal oxidation. In this context, a successful result is the oxidation of oxide forming elements (Al and Y) within the matrix of steel without the formation of Fe or Cr oxide scales.

In order to obtain this goal, the equilibrium oxygen partial pressures, i.e. the oxygen activities (a_{O_2}) at different temperatures for the oxidation of pure elements in the examined system (Fe, Cr, Al and Y) were calculated. The results versus inverse temperature (1000 K/T) have been plotted in figure 1. This plot is known as Ellingham diagram which is a fundamental tool for the understanding of the oxidation behavior of metals. Some selected temperatures in Celsius with vertical line have been shown in figure 1 as well. The thermodynamic databases used for this purpose were four databases referred as [13], [14], [15] and [16].

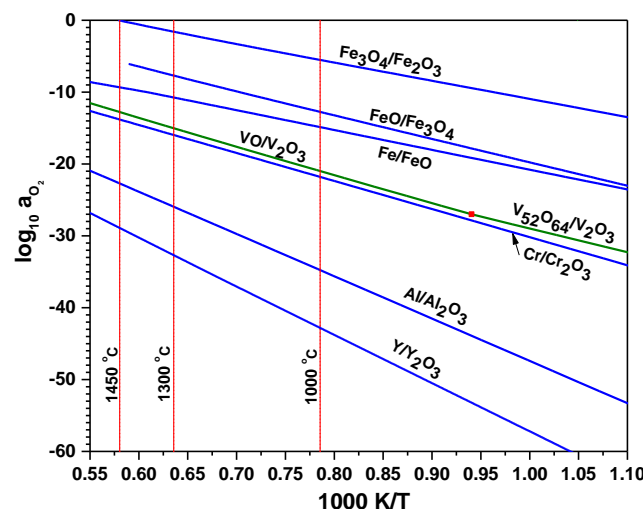


Figure 1. The calculated oxygen activity versus temperature for different metal/oxide equilibria.

It can be seen (figure 1) that at defined temperature for example at 1000 °C, the equilibrium reactions of (Al/Al₂O₃) and (Y/Y₂O₃) show lower oxygen activity data relative to Fe and Cr equilibrium oxidation reactions. This strengthens the possibility of internal oxidation in a steel alloy.

It should be reminded that in Ellingham type approach, the activities of metallic elements are equal to one, whereas the activity values of Fe, Cr, Al and Y in a real steel alloy are lower than one.

Moreover, this diagram (figure 1) was used to evaluate the oxygen buffer systems to fix the oxygen activities for the experiment. In this work, solid-state powder mixture to adjust the oxygen partial pressures for the purpose of this work was selected. To calculate the candidate buffer system, the dataset for the V-O system [17] in addition to the above stated databases was used.

The most important criterion for the choice of oxygen buffer system is the location of its equilibrium reaction line in the Ellingham diagram. The line has to be above (Al/Al₂O₃) and (Y/Y₂O₃) line and lower than (Fe/FeO) equilibrium line and ideally close to (Cr/Cr₂O₃) line. This is important since Al and/or Y has to be selectively oxidized relative to Fe and Cr as earlier noticed. Based on this concept, the equilibrium mixture of (VO/V₂O₃) seems to be a potential candidate for the purpose of internal oxidation (see figure 1). In this paper, the result of oxidation for a selected Fe-Cr-Al-Y alloy with this buffer has been reported.

3. Experimental procedure

A high purity alloy has been prepared by arc-melting in argon atmosphere (Ar 6.0). The starting materials were the metal pieces of Fe, Cr, Al and Y. The first three elements were 99.99% pure and Y was 99.9% pure. The metallic elements were all obtained from Alfa Aesar GmbH & Co KG.

The produced buttons were flipped and remelted five times in order to improve their homogeneity. Table 1 presents the composition of the alloy after its production which was determined by ICP-OES (Inductively coupled plasma-optical emission spectroscopy) method.

Table 1. The composition of the prepared alloy.

Alloy designation	Nominal composition (wt.%)				Chemical analysis (wt.%)			
	Y	Al	Cr	Fe	Y	Al	Cr	Fe
Fe-16Cr-0.2Al-0.05Y	0.05	0.2	16.0	83.75	0.0537	0.214	15.8	82.6

The chemical analysis (see Table 1) shows a good agreement with nominal compositions. The reported standard deviations (SD) for each element was acceptable as well ($SD_Y = 0.0011$, $SD_{Al} = 0.002$, $SD_{Cr} = 0.04$, $SD_{Fe} = 0.1$). In as-cast microstructure, the segregation of yttrium or aluminum was not detected.

Afterwards, a cube specimen from as-cast sample with a few millimeters size and a weight of approximately 1 g was produced. In order to standardize the surface conditions, all the sides of the specimens before the oxidation experiment were ground up to grade #4000 (SiC, Struers GmbH).

The oxidation step was performed by embedding the cube specimen into the selected equilibrium oxide powder mixture using (VO/V₂O₃) buffer system. The experiment was carried out for 20 h at 1450 °C.

The heating rate of the furnace from room temperature to the final temperature was fixed to ~ 4 °C/min. The experiment was performed under argon atmosphere (Ar 6.0). The starting constituents of the buffer and its oxygen activity at the defined temperature are given in Table 2. The equilibrium components of oxygen buffer mixtures (VO/V₂O₃) are expected to be formed during annealing (see Table 2).

Table 2. The composition of oxygen buffer system for the oxidation experiment described in this work.

Equilibrium components of oxygen buffer mixture	T(°C)	Provided oxygen activity ($\log_{10} a_{O_2}$)	Equivalent oxygen partial pressure (P_{O_2} in bar)	Starting constituents	Weight ratio of the starting constituents	Total weight
VO/V ₂ O ₃	1450	-12.8	1.61×10^{-13}	V/VO ₂	0.35 : 1	2 gr

The reason to carry out the experiments at high temperature and to put the alloy in direct contact to the buffer mixture is to make the kinetics of the transport of oxygen from the buffer to the alloy faster.

After the oxidation experiment, the specimen was cooled down to room temperature inside the furnace. The attached powders were then removed from the surface of specimen by mechanical grinding. The microstructure of the specimen was then imaged with scanning electron microscopy (SEM), FEIXL30S, coupled with EDX detector allowing spot and line scan analyses.

4. Results and Discussions

The result at higher temperature experiment (1450 °C) for Fe-16Cr-0.2Al-0.05Y by a direct contact of the alloy and powder mixture (VO/V₂O₃) for 20 h is shown in figure 2.

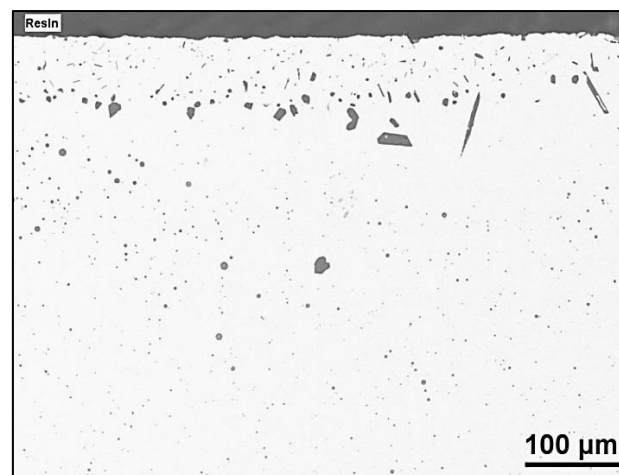


Figure 2. The internally oxidized zone Fe-16Cr-0.2Al-0.05Y with (VO/V₂O₃) buffer for 20 h at 1450 °C on a surface approximately through the middle of sample (after 2 mm grinding from one side). The images are cross-section backscattered-micrographs (magnification of 200x). The coarser oxide particles near the surface and finer oxide particles in the inner regions can be seen.

It can be seen that in outer regions of the sample, the coarser particles are present, whereas the finer particles in the inner regions have been formed. In fact two distinguishing varieties in the size of the particles can be observed. A typical EDX line scan profile for coarser particles is shown in figure 3.

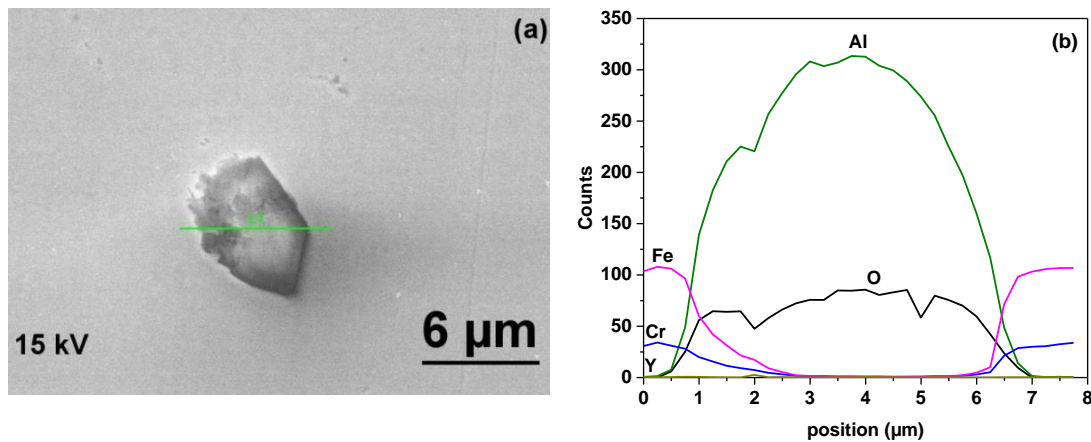


Figure 3. A typical EDX analysis for the coarser formed particles in Fe-16Cr-0.2Al-0.05Y at 1450 °C in outer regions of the sample after 20 h embedded in (VO/V₂O₃) oxygen buffer: (a) secondary electrons-micrograph and indicated path for line scan (magnification of 4800x), (b) the corresponding composition profile using 15 kV acceleration voltage showing the formation of aluminium-oxide particle.

As suggested by the EDX profile in figure 3, the coarser particles (with about a few micrometers size) are aluminum-oxide which are mostly near the surface of the specimen. The finer oxide particles (approximately some hundred nanometers) were located mainly in the interior of the sample consisting of mixed aluminum-yttrium oxides. This has been shown by an EDX line scan profile in figure 4.

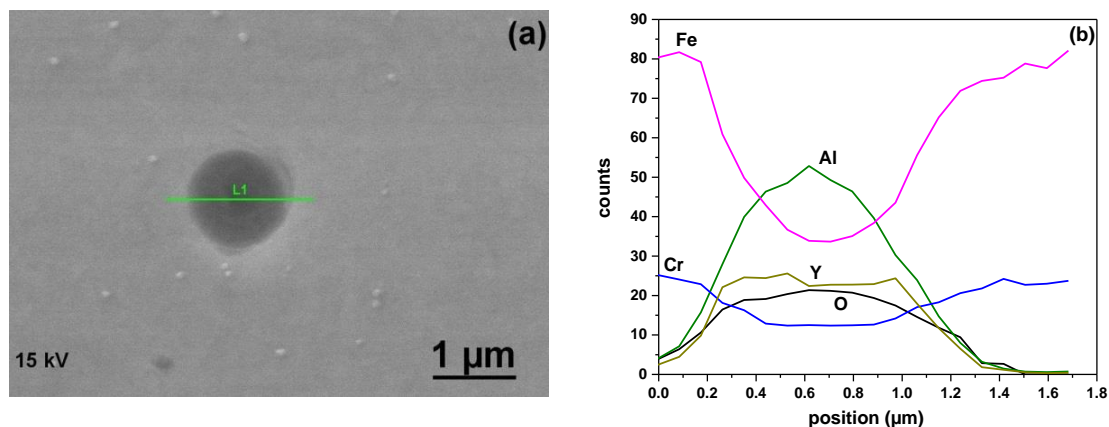


Figure 4 A typical EDX analysis for the finer formed particles in Fe-16Cr-0.2Al-0.05Y at 1450 °C located mainly in inner regions of the sample after 20 h embedded in (VO/V₂O₃) oxygen buffer: (a) secondary electrons-micrograph and indicated path for line scan (magnification of 20500x), (b) the corresponding composition profile using 15 kV acceleration voltage showing mixed aluminum-yttrium oxide particle.

It should be noted that the number of counts for Fe and Cr in the middle of path does not go down to zero (see figure 4b). This effect can be attributed to the small size of the particle which is in the range of the volume activated by the electron beam leading to contributions from the surrounding steel matrix. It is worth mentioning that the internal oxidation depth was approximately 2000 μm. The observed results are the successful internal oxidation examined steels by the formation of desirable

oxides particles (Al-O and Al-Y-O precipitates). External scales were not detected for the alloy as well.

5. Conclusions

The oxidation of Fe-16-0.2Al-0.05Y (wt.%) embedded into a (VO/V₂O₃) powder mixture at 1450 °C for 20 h led to an internally oxidized zone with a depth of about 2000 µm. The precipitates within this zone consisted of two types of oxides. Larger oxide particles (a few micrometers) were mainly formed near the surface and they were identified as aluminum oxide particles by EDX method. The finer oxide particles (approximately some hundred nanometers) were located mainly in the interior of the sample. They are identified as mixed aluminum-yttrium oxide particles.

At present, the oxide dispersions are still produced at relatively high temperatures and long oxidation times. As a result, the grain size of the matrix alloy and the particle sizes of the oxides are higher than in ODS steels produced by the powder metallurgical process. The oxide particles in these steels are still smaller by up to two orders of magnitude than in our alloys. Therefore we expect that in our ODS steels, the strengthening effect is clearly below that of the powder metallurgical alloys. Currently experiments are in progress to prepare by internal oxidation samples for tensile tests in order to determine the strengthening effect quantitatively.

Acknowledgement

The financial support of this work by the Helmholtz Alliance LIMTECH is gratefully acknowledged.

References

- [1] Shiba K, Tanigawa H, Hirose T, Sakasegawa H and Jitsukawa S 2011 *Fusion Engineering and Design* **86** 2895
- [2] Ehrlich K 2001 *Fusion Engineering and Design* **56-57** 71
- [3] Kimura A 2005 *Materials Transactions* **46** 394
- [4] Mao X, Kim T K, Kim S S, Han Y S, Oh K H and Jang J 2015 *Journal of Nuclear Materials* **461** 329
- [5] Lu C, Lu Z and Liu C 2013 *Journal of Nuclear Materials* **442** S148
- [6] Bruchhausen M, Turba K, De Haan F, Hähner P, Austin T and De Carlan Y 2014 *Journal of Nuclear Materials* **444** 283
- [7] Capdevila C, Bhadeshia H 2001 *Advanced Engineering Materials* **3** 647
- [8] Benjamin J S 1970 *Metallurgical Transactions* **1** 2943
- [9] Rieken J R, Anderson I E, Kramer M J, Odette G R, Stergar E and Haney E 2012 *Journal of Nuclear Materials* **428** 65
- [10] Xie R, Lu Z, Lu C and Liu C 2014 *Journal of Nuclear Materials* **455** 554
- [11] Wagner C 1959 *Zeitschrift für Elektrochemie* **63** 772
- [12] Rapp R A 1965 *Corrosion* **21** 382
- [13] TCFe7 TCS Steels/Fe-Alloys Database v7.0
- [14] Kjellqvist L, Selleby M and Sundman B 2008 *CALPHAD* **32** 577
- [15] TCBIN TC Binary Solutions Database v1.1
- [16] Swamy V, Seifert H J and Aldinger F 1998 *Journal of Alloys and Compounds* **269** 201
- [17] Yang Y, Mao H and Selleby M 2015 *CALPHAD* **51** 144